Primljen / Received: 5.1.2024.
Ispravljen / Corrected: 27.6.2024.
Prihvaćen / Accepted: 12.7.2024.
Dostupno online / Available online: 10.10.2024.

Method for upgrading isolated bridges with novel V gaped devices: Seismic tests of models

Authors:

[1]Assoc.Prof. Jelena Ristić, PhD. CE
jelena.ristic@ibu.edu.mk

[2]Ragip Behrami, MCE
rbehrami@gmail.com
Corresponding author

[3]Assoc.Prof. Zoran Brujić, PhD. CE
zbrujic@uns.ac.rs

[2]Prof. Danilo Ristić, PhD. CE
danilo.ristic@gmail.com

[2]Prof. Viktor Hristovski, PhD. CE
viktor@iziis.ukim.edu.mk

[1]International Balkan University (IBU), Skopje
Technical Faculty, Department of Civil Engineering
[2]University of St. Cyril and Methodius, Skopje
Institute of Earthquake Engineering and Engineering Seismology (IZIIS)
[3]University of Novi Sad, Serbia
Faculty of Technical Sciences

Original research paper

Jelena Ristic, Ragip Behrami, Zoran Brujic, Danilo Ristic, Viktor Hristovski

Method for upgrading isolated bridges with novel V gaped devices: Seismic tests of models

A method for enhancing the seismic performance of isolated bridges was developed using innovative vertical multigap (V-MG) devices based on extensive experimental and analytical research. Significant improvements in seismic performance were achieved by creating a unique type of uniform V-MG energy-dissipation device for a vertical-gaped bridge protection system (VG bridge system) that included double spherical rolling seismic bearings for seismic isolation as a complete set. Seismic shaking table tests on large-scale bridge models, which simulated real earthquake conditions, confirmed that the VG bridge system could significantly modify seismic response and enhance the seismic safety of isolated bridges under very strong earthquakes.

Key words:

bridge, model testing, energy dissipation, seismic isolation, seismic safety

Izvorni znanstveni rad

Jelena Ristić, Ragip Behrami, Zoran Brujić, Danilo Ristić, Viktor Hristovski

Metoda poboljšanja potresno izoliranih mostova novim V-MG uređajima: dinamička ispitivanja modela

Na temelju opsežnih eksperimentalnih i analitičkih istraživanja razvijena je metoda za poboljšanje odziva na djelovanje potresa izoliranih mostova uporabom inovativnih vertikalnih uređaja s višestrukim otvorima (V-MG). Znatna poboljšanja u svojstvima dinamičkog odziva na potres postignuta su razvojem jedinstvenog tipa V-MG uređaja za trošenje energije kao sustav zaštite mostova s vertikalnim razmacima (VG sustav mostova), koji je uključivao i dvostruke sferne kotrljajuće izolacijske ležajeve za potresnu izolaciju. Ispitivanja modela u velikome mjerilu na potresnom stolu, koja su simulirala stvarne uvjete potresa, potvrdila su da VG sustav mosta može znatno promijeniti dinamički odziv i povećati otpornost na potres izoliranih mostova uslijed vrlo jakih potresa.

Ključne riječi:

most, ispitivanje modela, trošenje energije, potresna izolacija, otpornost na potres

1. Introduction

Despite the recent intensification of contributions from numerous global studies on the seismic isolation of bridges that has led to a wide variety of concepts [1], most theoretical and experimental research is purpose-oriented and focuses on developing specific types of devices (rubber bearings, sliding bearings, rolling bearings, and displacement-limiting devices). Comprehensive reviews of the concepts and achievements in this field have been reported in [1, 2]. The hysteretic behaviours of commonly used rubber and lead-rubber seismic bearings have been analysed [3, 4]. The behaviours of sliding bearings have been studied through related research [5-7], and simple pendulum bearings have been studied [8-11]. Widely studied and applied isolation technologies [12] were supplemented with various dissipative mechanisms for protecting structures, particularly from near-source ground motion. Consequently, concepts and applications for developing additional devices for energy dissipation and large displacement-limiting devices have been introduced and investigated [13, 14]. The development of robust energy dissipation systems using inelastic steel deformation has been investigated in several studies [15]. Among them, U-shaped hysteretic steel dampers were primarily considered for buildings [16-18]. Tapered-steel energy-dissipation devices were introduced [19], and the principle of flexural beam dissipaters, either one- or multidirectional, have been extensively researched and applied [13, 20]. Recent advancements in this field have led to the development of novel materials [21, 22]. Studies also explored specific phenomena and concepts, such as pounding effects [23], axial behaviour of elastomeric bearings [24], and semi-active dampers [25, 26]. Design regulations for seismically isolated bridges have been introduced gradually [27, 28], continuously improved, and implemented globally, particularly in seismically active regions [29]. Further, complex systems have been studied frequently using shaking-table tests on the scaled structure models [30].

However, significant seismic damage to bridges are consistently observed after major earthquakes, indicating the inadequate resistance of bridge bearings, insufficient design of super- or substructures, and issues with foundation design. Within a bridge substructure, damage manifests as excessive deformations, settlements, permanent displacements, large cracks, or overturning of the structure [31-33], while the superstructure often experiences significant displacement, large cracks, or even collapse [34]. Modern bridges are not immune to the severe damage caused by strong earthquakes [35, 36]. Common design flaws observed in practice include neglecting relevant factors in creating safe solutions using energy dissipaters designed to act in only one direction, inconsistencies with the nature of earthquakes, and a lack of technological solutions for limiting very large displacements. Although many studies have confirmed the favourable behaviour of seismically isolated bridges worldwide, the number of near-fault bridges that experienced strong earthquakes is very low [35, 37]. Recent reports highlighted potential problems and less favourable behaviours. Abrupt damage to a seismically isolated bridge that withstood total collapse was observed on the large Bolu viaduct after the strong Duzce (Turkey) earthquake in 1999 because of the ruptured fault crossing the viaduct and earthquake being significantly stronger than the designed one [38, 39]. Similarly, during the 1995 Kobe earthquake, the Higashi-Kobe Bridge suffered damage related to large displacements [40], and several isolated bridges were reported to have been damaged during the Great East Japan Earthquake in 2011. Smaller-scale damage was reported on the Thjorsa River Bridge and Oseyrar Bridge in Iceland after a near-fault ground motion [41].

This study aims to develop a more efficient bridge protection technology to address the need to minimise intolerable earthquake damage to common and modern bridges. This paper presents innovative research segments and the basic concept of a new VG bridge system developed for the efficient seismic protection of bridges exposed to strong abrupt earthquakes.

2. Study objectives and concept of the VG bridge system

2.1. Study objectives

This study focuses on developing and testing a novel VG bridge system representing a segment of a wider long-term research project. The VG bridge system was enhanced by upgrading the conventional isolated bridge system with the newly developed uniform all-directional vertical multigap (V-MG) energy dissipation (ED) devices. Therefore, the VG bridge system embodies an advanced upgrading method based on installing adaptive passive mechanical devices that provide harmonised response modifications for bridge structures during strong earthquakes. This comprehensive long-term innovative study, which involves extensive experimental and analytical research, was successfully conducted at the Institute of Earthquake Engineering and Engineering Seismology (IZIIS), Ss. Cyril and Methods University, Skopje, Republic of North Macedonia. The integral research activities were conducted in the frames of the supported innovative NATO Science for Peace and Security Project *"Seismic Upgrading of Bridges in South-East Europe by Innovative Technologies",* which involved five countries and was led by the fourth author as the Partner Country Project Director (PPD) at IZIIS, Skopje.

2.2. Concept of the VG bridge system

The VG system demonstrates the unique ability for the global optimisation of the seismic energy balance by incorporating the novel V-MG energy dissipation devices as supplementary damping for the isolation of bridge superstructures. The VG bridge comprises three essential and complementary systems.

1. **SI system:** The seismic isolation (SI) system offers low horizontal stiffness while safely supporting the weight of the

superstructure. Properly designed seismic isolators can be installed at each support point of the bridge superstructure by transferring the weight to middle piers and/or rigid abutments. Various seismic isolation devices can be implemented, including those used in this study.

2. **ED system:** Unlike isolators, a seismic energy dissipation (ED) system provides sufficient damping to dissipate seismic energy. The ED devices achieve high energy-dissipation capacity because of their nonlinear behaviour and hysteretic properties. They must be optimally designed considering the performance of seismic isolators. The requirements include optimal stiffness to prevent inertial impulse forces, a bearing capacity set to design a limit to avoid large inertial forces on the piers, and sufficient ductility for enduring large deformations before damage. The proposed all-directional uniform vertical multigap (V-MG) energy-dissipation devices achieved significant advancements in these areas.
3. **Displacement limiting (DL):** During severe earthquake vibrations, several strong inertial force impulses accompanied by large displacements can occur. Such excessive displacements cannot be reliably controlled using standard engineering methods. The proposed displacement-limiting system with specific DL devices can mitigate or eliminate strong impact effects.

Innovative research can be divided into two categories. The first section focuses on the development, testing, and modelling of new uniform V-MG energy-dissipation components and devices required for a large-scale VG bridge prototype testing model. The second section describes the seismic testing of the VG bridge model under simulated intense earthquake conditions using IZIIS seismic shaking table equipment. The physical VG bridge model was meticulously designed and built to ensure effective performance during both quasi-static testing of components and devices and the shaking table tests.

3. Created uniform V-MG energy dissipation devices

3.1. Concept of V-MG device

Given the specific objective of this study, specific attention was devoted to creating an integrated and compact unit with a highly ductile response. This innovative unit is a vertical multigap (MG) and multidirectional (MD) energy dissipation device (V-MG device) with a significant capacity for seismic energy dissipation. The multidirectional V-MG energy-dissipation device, illustrated in Figure 1, includes a base metal plate for fixing vertical components, vertical energy-dissipation components (EDCs), and an upper metal plate featuring two rings of gap openings, both inner and outer. The activation modes of the device are designed to adapt to frequent weak earthquakes, numerous stronger earthquakes, and rare but potentially destructive earthquakes. The developed ED prototype devices were produced through a design process that ensured consistent characteristics for all constituent parts.

The base plate (1) was manufactured to be circular, d = 25 mm thick, and a metal plate with a diameter of D = 450 mm (Figure 1). Eight (per circle) uniformly spaced fixed-diameter holes with windings distributed along two concentric circles (inner and outer circles with diameters d1 = 190 mm and d2 = 340 mm) were manufactured for fixing vertical ED components (2) and (4). The walls of all holes were chamfered (6.9 mm in depth, 30° angle) to avoid the rocker effect during horizontal deformation. The vertical ED components were made of ductile metal (S355 steel class) and shaped like cut cones (Figure 1). Based on the

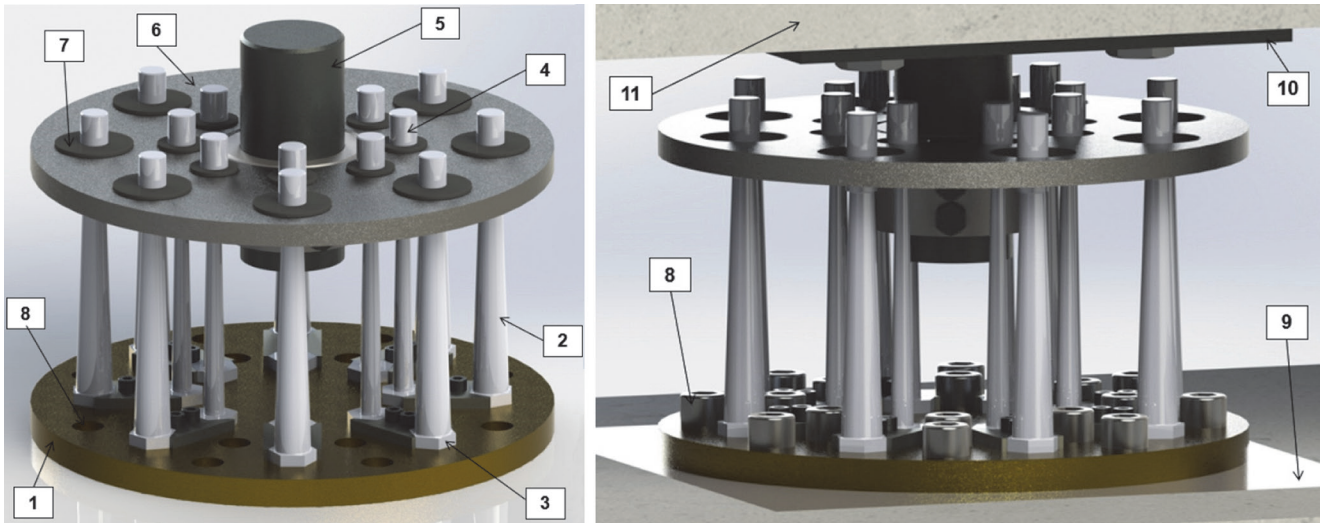

Figure 1. Designed V-MG device: 1. Base fixing plate; 2. Outer dissipation components; 3. Fixing segment; 4. Inner dissipation components; 5. Activation body; 6. Activation plate; 7. Gap-distance protector; 8. Fixing bolts to sub-structure; 9. Bridge sub-structure; 10. Fixing plate to super-structure; and 11. Bridge super-structure

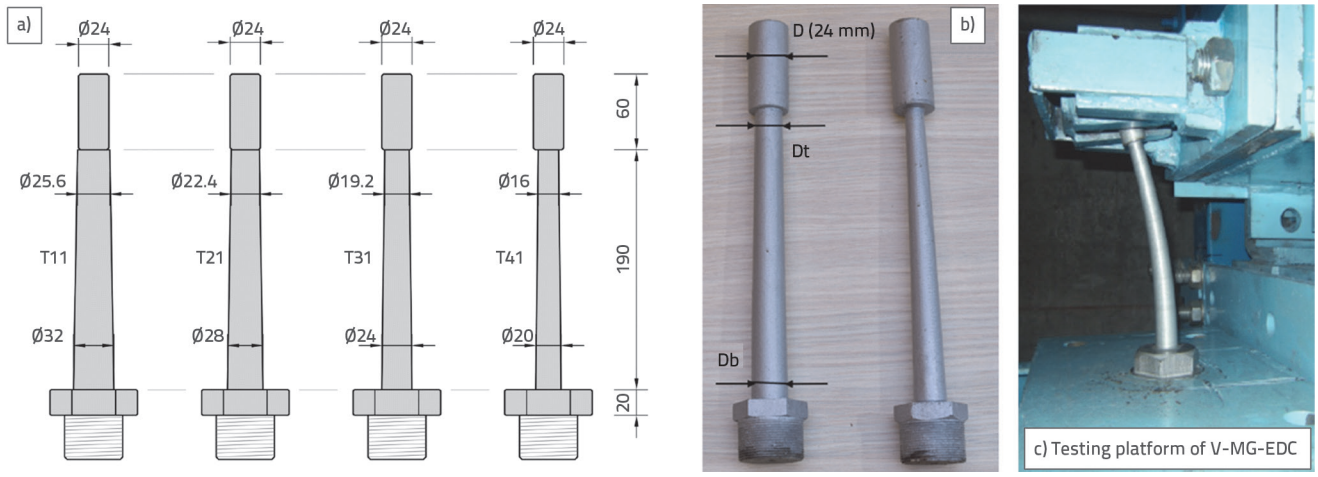

Figure 2. V-MG components: a) Geometry; b) Manufactured components; and c) Testing platform for components

bottom cone diameter (Db), four prototype types of ED devices were adopted (Db = 32, 28, 24, and 20 mm), each available in two variants differing in the top cone diameter (Dt), as shown in Table 1, which includes the geometry form notation. Further, each vertical component had a cone body height of 190 mm and ended with a cylindrical part that was 60 mm long (h2) and 24 mm in diameter (Figure 2). This geometry enables the component to be fixed to the base plate, whereas the cylindrical top provides gap-G1 and gap-G2 conditions for the gap-based activation.

The activating circular plate (6), which was 20 mm thick, was designed with two concentric rings of gap holes (Figure 1): eight holes along the inner circle (d1 = 190 mm) with a diameter of 34 mm and eight holes along the outer circle (d2 = 340 mm) with a diameter of 60 mm. Each hole accommodated a cylindrical part with a diameter of 24 mm, providing a gap of 5 mm (G1) for the inner holes and 18 mm (G2) for the outer holes in all directions.

A unique and compact V-MG energy-dissipation device was formed by assembling all three segments. As described previously, this device structure enabled adaptive activation corresponding to the intensity of earthquakes, which is achieved through the sequential activation of components installed with varying gap sizes.

3.2. Testing the performances of V-MG components

The prototypes were tested under simulated quasi-static loads before integrating the V-MG devices into the bridge model for shaking-table testing. The quasi-static test program included reversed cyclic testing in three stages: (1) seismic isolation of the DSRSB devices, (2) energy-dissipation device components, and (3) fully assembled energy-dissipation devices. As illustrated in Figure 3b, the same quasi-static loading protocol used for SI devices was applied. Each V-MG component underwent two tests: an initial test (test-1) to establish hysteretic response under initial conditions and a repeated test (test-2) for evaluating the stability and consistency of the hysteretic response observed in the initial test.

Each of the eight V-MG components was separately tested under a quasi-static load using specific dedicated equipment (Figure 2c), which simulated the boundary conditions of the component, the provided G1 (5 mm) or G2 (18 mm) gap, and the gapless conditions. Thus, an extensive volume of data—the hysteretic gap, non-gap-based responses, and high energy dissipation performances for all V-MG components–was obtained [42]. Figure 4 shows two selected hysteretic responses for component T11 for the two gap sizes. The

Table 1. Prototype models of VG-ED components

Prototype type	Prototype notation	Geometry form	Geometry of gaps	Activation direction	Base – Db [mm]	Top – Dt [mm]
1	V-MG-MD-T11	T11	G1 i G2	MD	32.0	25.6
	V-MG-MD-T12	T12	G1 i G2	MD	32.0	19.2
2	V-MG-MD-T21	T21	G1 i G2	MD	28.0	22.4
	V-MG-MD-T22	T22	G1 i G2	MD	28.0	16.0
3	V-MG-MD-T31	T31	G1 i G2	MD	24.0	19.2
	V-MG-MD-T32	T32	G1 i G2	MD	24.0	14.4
4	V-MG-MD-T41	T41	G1 i G2	MD	20.0	16.0
	V-MG-MD-T42	T42	G1 i G2	MD	20.0	12.0

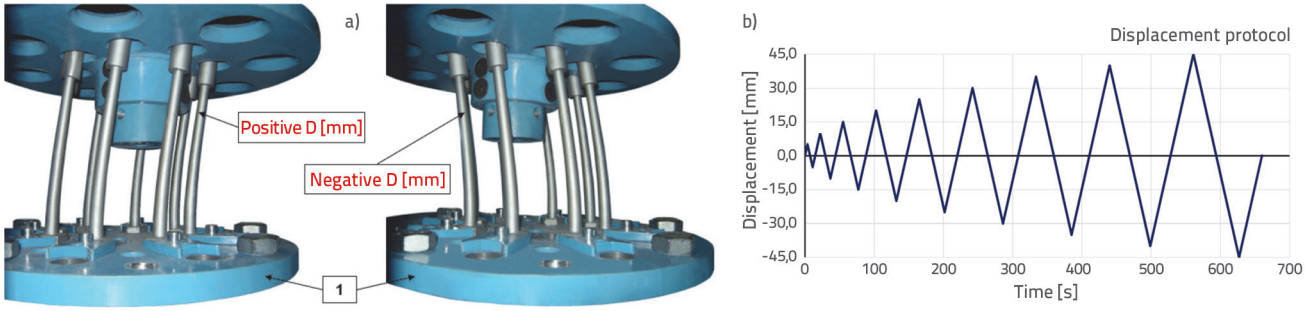

Figure 3. Cyclic testing: a) Imposed positive and negative displacement; b) Displacement protocol

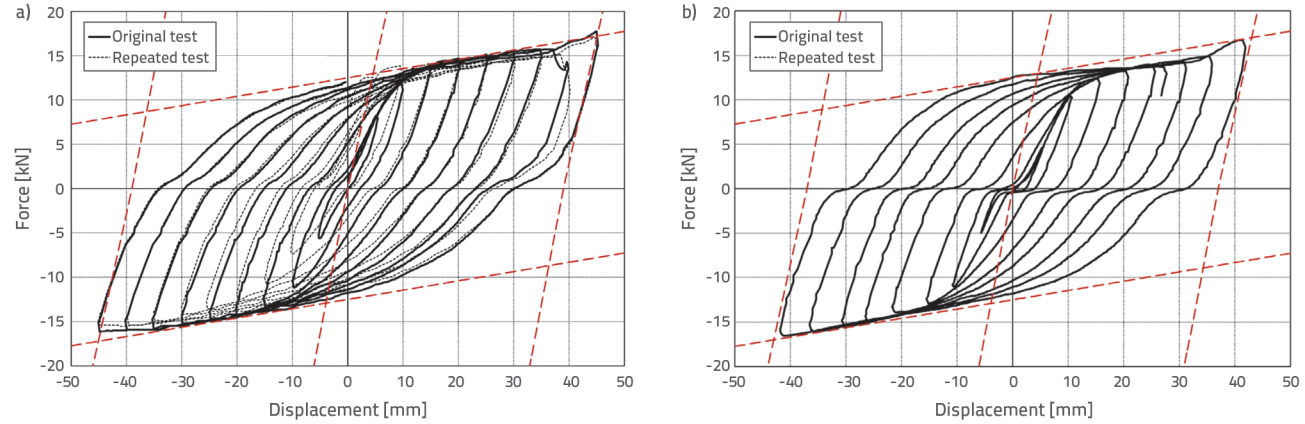

Figure 4. Response of two components type V-MG-MD-T11: Gapless (left) and gap G1 = 5 mm (right)

parameters determining the hysteretic response were the same in the two-gap cases when the yield force and displacements were considered. The repeated tests resulted in an insignificant decrease in the yielding force.

In the experimental study, the observed hysteretic responses of the V-MG components remained highly stable throughout the original and repeated test sequences (Figure 4, left). The hysteresis shape, which varied noticeably with the gap size, was effectively modelled using a simple bilinear model (Figure 4). Finally, the V-MG device demonstrated adaptable nonlinear behaviour and substantial energy-dissipation because of its stable multigap and multidirectional hysteretic response.

3.3. Refined analytical modelling of V-MG components

An analytical simulation of the distinct gap-based hysteretic behaviour of the V-MG prototype components was conducted for exploring the potential of theoretically predicting the nonlinear behaviour of these devices. The successful application of such analyses could serve as virtual experiments, revealing the characteristics of future systems or modifications based on similar concepts.

As shown in Figure 5 (left), an advanced microanalytical model precisely representing the geometry of the integral

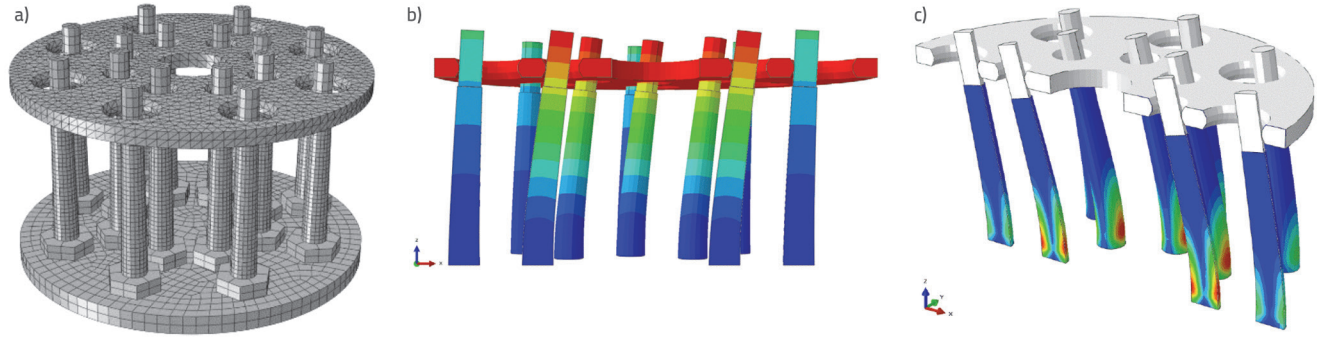

Figure 5. Abaqus micromodel of the full V-MG-ED device and component-type V-MG-MD-T11: FEM model (left); Deformed model when the top plate displacement reaches 25 mm (Cut view middle); Plastic deformation in components when the top plate displacement reaches 45 mm (Cut view right)

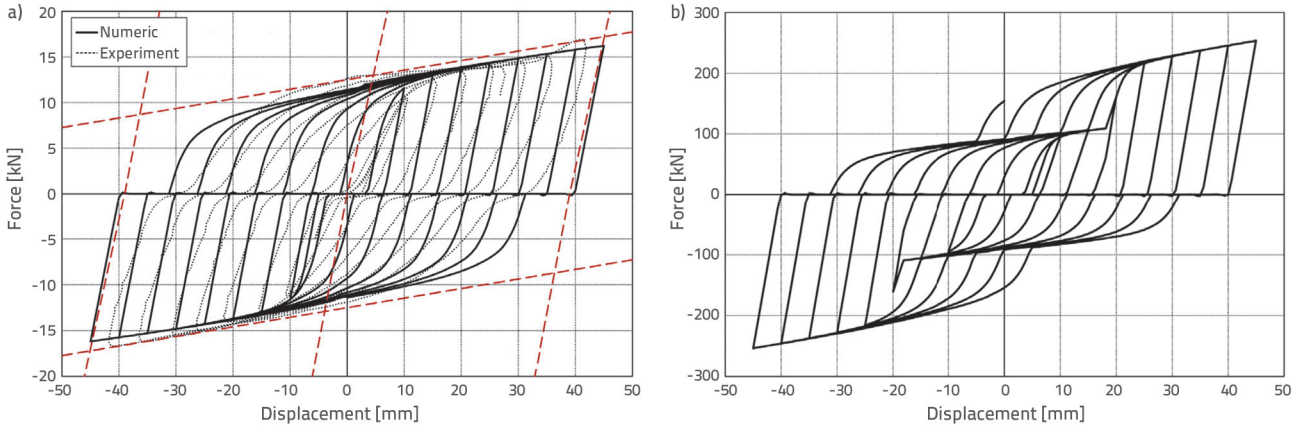

Figure 6. Computed hysteretic responses: a) Single T11 component installed with gap G1 = 5 mm; b) Single ED device with 16 T11 components installed with gaps G1 = 5 mm and G2 = 18 mm

ED device was formulated using the Abaqus computer software. Fixed boundary conditions were applied to the bottom surface for simulating quasi-static testing correctly, whereas the same horizontal displacement protocol was imposed on the upper surface, as shown in Figure 5 (middle). Material properties related to the steel used in the S355 class were attributed to all modelled elements; however, the plates and cylindrical top parts of the components were modelled for linear-elastic behaviour to increase the calculation efficiency, whereas nonlinear material properties were used for the variable-width parts, which included a bilinear kinematic hardening material model. The conditions for testing the components are met by suppressing the individual components, while a slightly modified model may provide gapless conditions. As an illustration, the predicted deformed shape of the components and distribution of the equivalent plastic deformation for two different imposed displacement values are presented in Figure 5 (middle and right).

As illustrated in Figure 6 (left), a very good match between the experimental and numerical results was achieved [42] by comparing the numerically obtained plot for one gapped (G1 = 5 mm) T11 component with the experimentally obtained one. Finally, a numerically obtained force–displacement hysteretic response of the entire device (Figure 5 (left)) is plotted in Figure 6 (right). The resulting plot of the device corresponded to the sum of the component responses because of the mutually independent deformations of the ED components. Experimental and analytical studies indicated that V-MG devices exhibited a stable and advanced hysteretic response along with effective energy-dissipation characteristics.

4. Prototype models of seismic isolation and displacement limiting devices

The SI system implemented in the VG bridge model utilised the prototype models of double-spherical rolling seismic bearing (DSRSB) devices originally designed for reuse across various planned experimental phases [42]. The DSRSB devices were engineered to offer a substantial vertical bearing capacity and significant displacement capacity. Spherical surfaces with a radius of 1000 mm were tailored to match the targeted vibration period, ensuring a minimal frictional reaction on the sliding surfaces. Figure 7 illustrates the geometry and components of the DSRSB device, which features spherical plates made from hard inox polished to a mirror shine for reducing friction and enhancing durability. The rolling element comprised a ring of balls with diameters of 12–18 mm arranged around a cylindrical slider.

Quasi-static testing of the bridge isolation devices involved mounting four DSRSB devices at the designated positions within the bridge prototype model (Figure 10) with two devices at each end support. An RC superstructure slab, weighing 85 kN, applied a vertical force of 21.25 kN to each device. A displacement-controlled cyclic loading protocol with amplitudes of up to 45 mm was employed for all quasi-static tests. As depicted in Figure 9 [43], an originally developed actuator applies a load onto the superstructure slab.

Figure 8 shows the characteristic hysteretic response of a single DSRSB device, which demonstrates a sufficient horizontal deformation capacity of up to 40 mm, stable hysteretic behaviour, and minimal frictional reaction. The shape of the hysteresis loops resembled a skewed rectangle, which was effectively represented by a bilinear model (Figure 8).

A displacement limitation (DL) system was engineered to mitigate any risk associated with the potential collapse of the superstructure of the bridge model during intense dynamic responses and ensure the overall test safety in simulated severe earthquakes. This DL system integrates eight dedicated limiting devices designed as short flexible steel cantilevers supported by rubber blocks (depicted in Figure 9, 6, and 10) functioning as nonlinear stoppers. These devices were strategically positioned at a suitable gap distance and

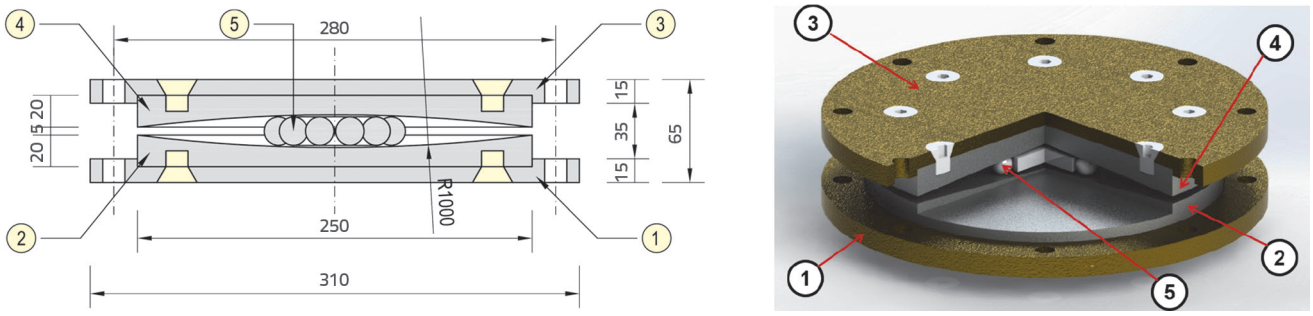

Figure 7. Prototype model of DSRSB seismic isolation device, cross-section, and visualisation: 1. Lower end plate; 2. Lower spherical plate; 3. Upper end plate; 4. Upper spherical plate; and 5. Central rolling part

aligned with ED devices, ensuring activation only under conditions of excessive displacement.

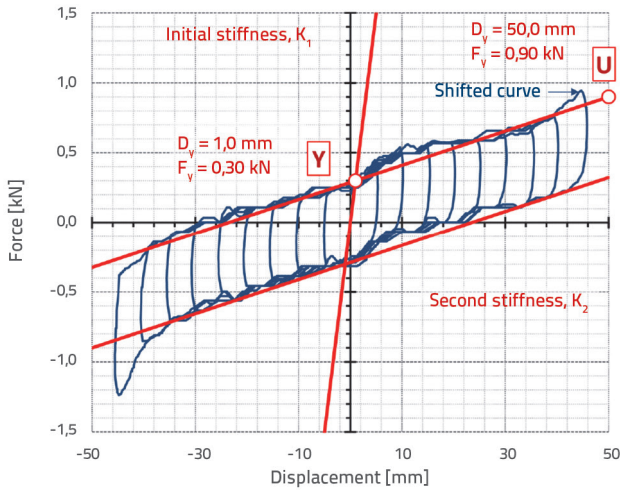

Figure 8. Hysteretic response of a single DSRSB isolation device

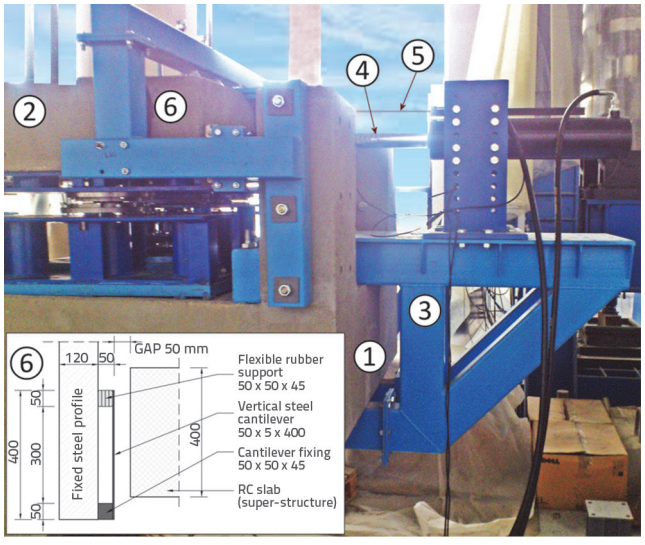

Figure 9. Actuator structure (re-used system)

5. Seismic testing of the VG bridge prototype model

5.1. Construction of the VG bridge prototype model

Dynamic testing was conducted using a specially designed large-scale VG bridge model that provided realistic conditions for the experimental simulation. The prototype bridge was selected to meet the requirements for the typical configuration and suitability for enhancement: a three-span bridge with two rigid abutments and two flexible mid-piers, totalling 58.5 m in length (15.75 m + 27.0 m + 15.75 m). The piers varied in height (9.50 and 11.70 m). The reinforced concrete (RC) deck of the bridge, spaced from the substructure to accommodate the VG system devices, was supported by movable bearings at the abutments and hinged connections on the piers.

The experimental model, ISUBRIDGE VG test model (Figure 10), was geometrically scaled down (1:9 scale factor) from the prototype bridge to match the dimensions and load capacity of the shaking-table equipment [44, 45]. The abutments and substructure base were designed and constructed as highly rigid reinforced concrete (RC) elements, while the middle piers were fabricated from steels of varying heights to provide flexibility. The superstructure was a rigid deck with an increased height to accommodate additional loads and simulate the significant inertial forces necessary for activating the VG system.

The model functioned as a single-span structure in configurations in which mid piers were not utilised. The steel components were made of S355 steel, and concrete C25/30 was used for all RC parts of the bridge model. The model is designed as a versatile platform to test various innovative bridge isolation systems.

The geometry of the bridge model is illustrated in Figure 11. The substructure comprised two parallel rigid RC knee beams (Figure 11, Part 1) with variable rectangular cross sections (25/50 cm and 25/70 cm) for accommodating different mid-pier heights, totalling 8.30 m in length. The sloped-ends extend beyond the edges of the shaking table to provide elevated abutment support. Horizontal sections of these beams measured up to 5.20 m in length and 1.50 m in width, enabling the bridge model to rest diagonally on the table.

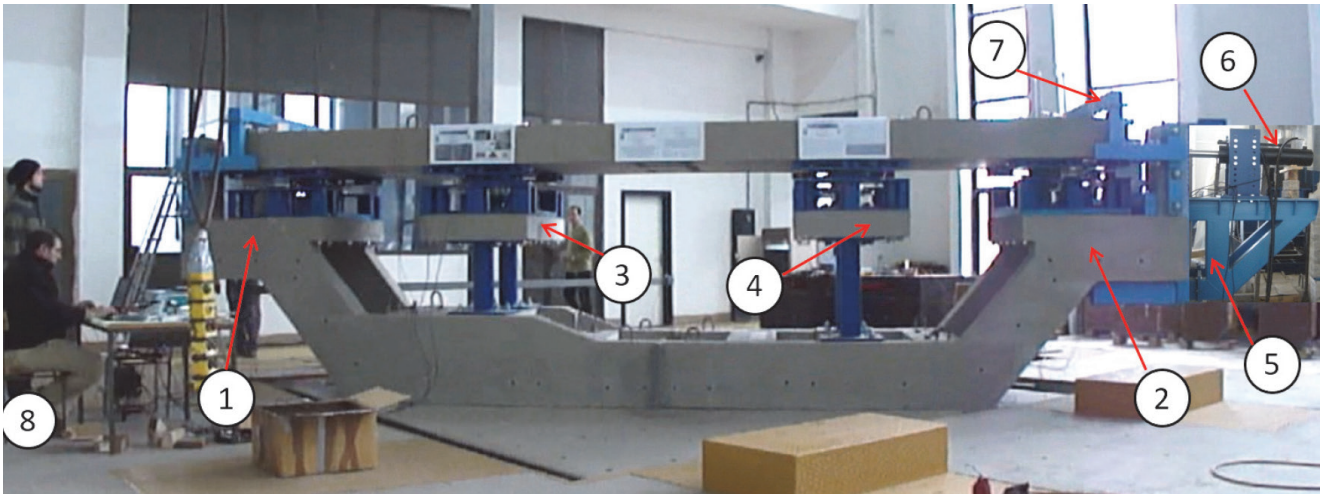

Figure 10. ISUBRIDGE model on the IZIIS shaking table (re-used prototype): 1. Left end support; 2. Right end support; 3. Support above shorter piers; 4. Support above longer piers; 5. Actuator supporting structure; 6. Actuator; 7. support of DL devices; and 8. Computer controlling the cyclic tests

Six transverse beams connected the two knee beams at the base (Parts 2, 3, and 4) with two beams (Part 3) supporting the mid piers. In addition, two beams (Part 5) were positioned at the elevated ends of the knee beams, and two monolithic cast-in-place slabs (Part 6) served as platforms for installing the devices (Figure 12). Short RC columns (Part 7) were placed at the ends of the beams as safety elements for controlling large displacements.

The middle piers (Part 8) were constructed from steel tubes (outside diameter of 168 mm and wall thickness of 12 mm) arranged in pairs of columns. Steel plates welded to the upper ends of the tubes supported the RC slabs (parts 9; 90 cm × 150 cm with a thickness of 20 cm), providing additional platforms for device mounting. The substructure was prefabricated into two parts and later connected using front steel plates and bolts because of the limitations of the laboratory crane.

The superstructure of the test model consisted of an RC deck (part 10) with a cross-section of 150 cm × 30 cm, spanning 740 cm in length with 20 cm gaps from the vertical short columns at both ends.

The deck was positioned 40 cm above substructure slabs to fit steel spacers attached to RC plates of both the substructure and superstructure. Displacement limitation (DL) devices used during testing were vertical flexible steel cantilevers, each 400 mm long, fixed at one end and supported by a 50 mm × 50 mm rubber block at the upper end (as shown schematically in Figure 9, part 6). These devices were placed 50 mm away from the RC superstructure to prevent excessive displacements. For the dynamic testing of the VG system, a one-span model setup was utilised (Figure 12), with the RC deck supported by two pairs of DSRSB isolators (Figure 7) installed only at the abutments (parts 1-4). The V-MG devices (Figure 1) were positioned along the longitudinal axis of the bridge model at the abutments between the substructure end slabs and the deck (parts A and B). These V-MG devices comprised V-MG-MD-T11 type energy dissipation components. Eight components were installed across the two levels, with four components radially distributed per level, designed to accommodate two predefined gaps: G1 = 5.0 mm and G2 = 18.0 mm.

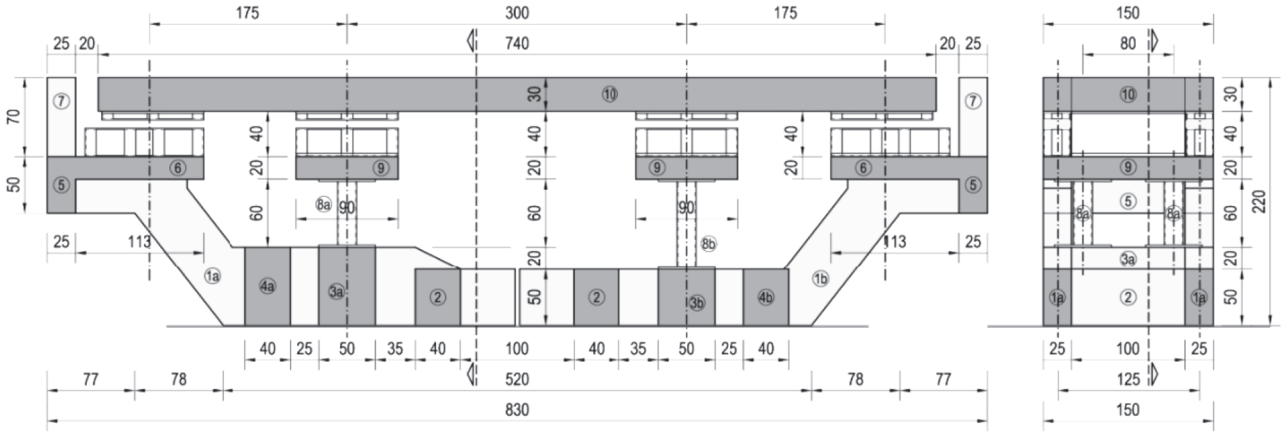

Figure 11. ISUBRIDGE bridge test model geometry: Longitudinal and transverse sections

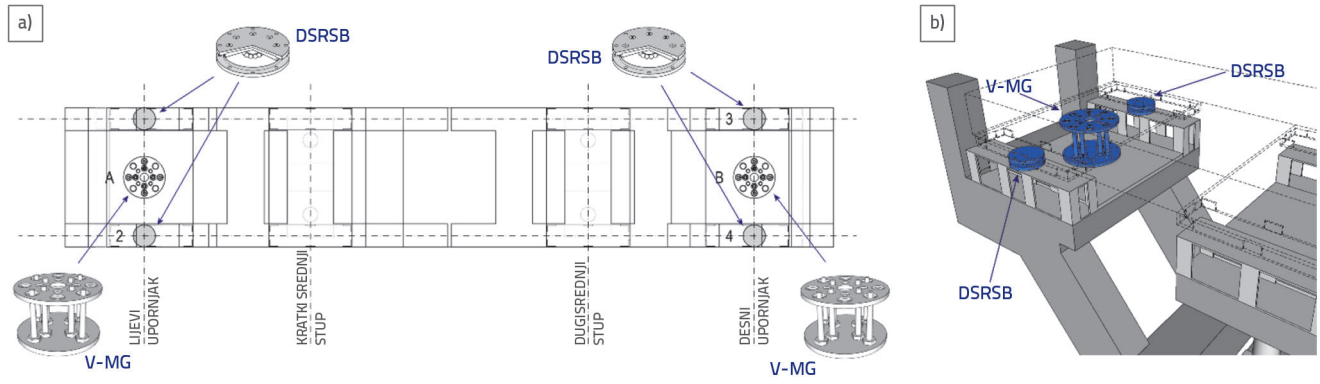

Figure 12. Dynamic test setup: (a) top-view positions of the four DSRSB devices (1–4), two V-MG devices (A and B), and (b) installed devices at the left abutment (perspective view)

5.2. Setup of VG prototype model on seismic shaking table

The seismic shaking table utilised in the experiment featured a square-shaped platform (5.0 × 5.0 m) capable of applying seismic input horizontally and vertically. The model was positioned diagonally on the platform to align it with the dimensions of the shaking table (Figures 10 and 13). This arrangement not only maximises the available space but also facilitates the generation of seismic forces in both the longitudinal and transverse horizontal directions of the model, thereby ensuring a realistic simulation of earthquake motion conditions.

5.3. Instrumentation of the VG seismic testing model

The instrumentation of the USI-V bridge model, which excludes additional channels for controlling the shaking table, incorporated three types of sensors for ensuring comprehensive data acquisition during dynamic tests (Figure 13), and a set of four LVDT transducers (LVDT-01 to LVDT-04) placed at two nodal points to record the time histories of the relative horizontal displacements (longitudinal and transverse separately) between the substructure and superstructure.

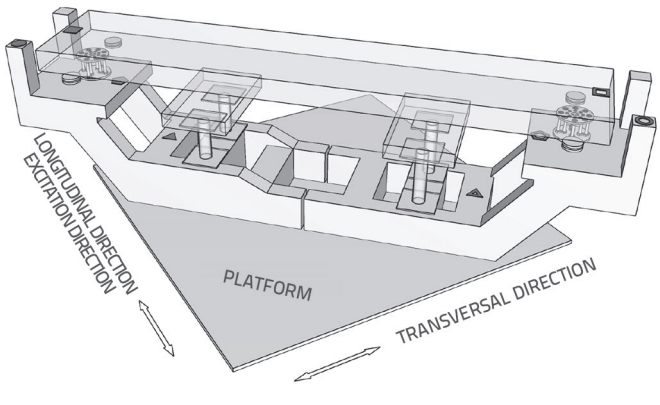

CH 01	NP 1	⬟	L	LVDT-01
CH 02	NP 1	⬟	T	LVDT-02
CH 03	NP 2	⬠	L	LVDT-03
CH 04	NP 2	⬠	T	LVDT-04
CH 05	NP 3	▲	L	LP-01
CH 06	NP 4	△	T	LP-02
CH 07	NP 7	■	L	LP-03
CH 08	NP 8	□	T	LP-04
CH 09	NP 3	■	L	ACC-01
CH 10	NP 3	■	T	ACC-02
CH 11	NP 4	□	L	ACC-03
CH 12	NP 4	□	T	ACC-04
CH 13	NP 5	●	L	ACC-05
CH 14	NP 5	●	T	ACC-06
CH 15	NP 6	○	L	ACC-07
CH 16	NP 6	○	T	ACC-08
CH 17	NP 7	▲	L	ACC-09
CH 18	NP 7	▲	T	ACC-10
CH 19	NP 8	△	L	ACC-11
CH20	NP 8	△	T	ACC-12

Figure 13. Acquisition points and used sensors with the respective recording channels (re-used system); L – longitudinal, T – transversal, NP – nodal point

These sensors monitor the activation of the DSRSB and V-MG devices in response to the induced relative displacements. Four linear potentiometers (LP) were installed to capture the time histories of absolute longitudinal displacements at four designated points. LP-01 and LP-02 measured the longitudinal displacement of the platform relative to the platform itself, while LP-03 and LP-04 monitored the superstructure motion. ACC sensors were employed to record the time histories of accelerations at six specific points across the model. Each point recorded the longitudinal and transverse components totalling 12 channels: ACC-01–ACC-04 for the superstructure acceleration, ACC-05–ACC-08 for the upper substructure, and ACC-09–ACC-12 for the lower substructure acceleration.

5.4. Seismic testing program for the VG bridge prototype model

All characteristics of the dynamic tests, except for the model geometry, had to be properly scaled to preserve the specific design concept. Considering primary factors, the combined true replica-artificial mass simulation model was considered the most appropriate. Scale factors for various physical quantities are specific functions of the geometrical scale factor based on the similitude law [46]. Prior to seismic testing, multiple sine sweep tests were conducted for identifying the damping and resonant frequencies of the model. These tests used simulated sine sweep inputs with moderate strengths (0.02 and 0.05 g) covering frequencies from 1–35 Hz. They provided essential data for determining the initial fundamental vibration period of 0.48 s (approximately corresponding to the fundamental period of the prototype bridge of 1.5 s), under conditions where only DSRSB devices were active (V-MG devices were not engaged due to existing gaps).

Table 2. Recorded positive and negative peak relative displacements for LVDT-03 and LVDT-04 in the two LVDT channels

Simulated earthquake	LVDT-03		LVDT-04	
	Max. + [mm]	Max. – [mm]	Max. + [mm]	Max. – [mm]
El-Centro, PGA = 0.78 g	26.04	17.96	6.55	2.23
Northridge, PGA = 0.89 g	31.61	29.94	4.56	6.44
Landers, PGA = 0.76 g	11.76	20.35	3.38	1.78
Petrovac, PGA = 0.72 g	15.22	26.61	2.52	1.59

Table 3. Positive and negative peak accelerations were recorded for three ACC channels: ACC-01, ACC-03, and ACC-05

Channel	El-Centro, PGA = 0.78 g				Petrovac, PGA = 0.72 g			
	Max. [g]	Dynamic amplification factor (DAF)	Maks. [g]	Dynamic amplification factor (DAF)	Max. [g]	Dynamic amplification factor (DAF)	Max. [g]	Dynamic amplification factor (DAF)
ACC-01	0.88	112.8%	0.74	94.9%	0.59	81.9%	0.45	62.5%
ACC-03	0.99	126.9%	1.15	147.4%	1.25	173.6%	1.40	194.4%
ACC-05	0.73	93.6%	0.62	79.5%	0.48	66.7%	0.67	93.1%

A damping ratio between 3.0 and 3.5% was observed when the complete VG system was activated for stronger sine-sweep inputs. Seismic input programming was designed to generate data relevant to the objectives of the study by leveraging seismic records representative of dynamic conditions close to critical scenarios for a non-isolated prototype bridge type (with a fundamental period of ~0.5 s).

The seismic testing of the bridge model was conducted using four earthquake records: El-Centro (1940), Northridge (1994), Landers (1992), and Petrovac (Montenegro, 1979). The original earthquake records were compressed by a time factor of 1/3 (root of the geometric scale, 1/9) to adjust the frequency content of these records to match the dynamic characteristics of the scaled test model. The ground accelerations used were 0.78, 0.89, 0.76, and 0.72 g for El-Centro, Northridge, Landers, and Petrovac, respectively.

Each seismic test was conducted twice for generating the original and repeated sets of records. The comprehensive data acquisition system included 20 instrumented channels aligned with the model instrumentation plan, along with common channels for platform control, which results in the collection of approximately five million numerical data points per test. The testing process was successful, with all sensors delivering continuous and accurate experimental records. The results are presented in the following tables and charts.

Table 2 summarises the peak positive and negative values of relative displacements in the longitudinal and transverse directions as recorded by LVDT sensors positioned at the right abutment (channels LVDT-03 and LVDT-04, respectively) across all four earthquake simulations. As shown in Figure 14 (left charts), the time-history plots of the superstructure relative displacements captured by LVDT-03 (longitudinal) and LVDT-04 (transverse) during tests replicating the strong El Centro, Northridge, and Petrovac earthquakes are depicted. Further, LVDT-03 recorded dominant displacements aligned with the earthquake direction, while LVDT-04 registered smaller and lower less significant displacements perpendicular to the excitation.

The maximum absolute relative displacement observed was 31.61 mm during the intense Northridge earthquake simulation, which remained below the critical allowable displacement limit of 40.0 mm for DSRSB seismic isolators. Seismic responses of the VG system were highly consistent between the original and repeated shaking table tests, thereby indicating negligible differences in peak relative displacements.

Table 3 displays the representative peak acceleration values recorded by sensors ACC-01, ACC-03, and ACC-05 in the longitudinal direction during the shaking table tests under simulated strong El Centro and Petrovac earthquakes. Further, these values are presented relative to the input peak ground acceleration, which indicates the dynamic amplification factor (DAF). Figure 14 (right charts) illustrates the time-history plots of responses recorded by the ACC-03 (longitudinal) and ACC-04 (transverse) sensors during tests replicating the El Centro, Northridge, and Petrovac earthquakes.

ACC-03 recorded dominant accelerations aligned with the earthquake direction, whereas ACC-04 recorded smaller transverse accelerations. The accelerations at the substructure nodal points are smaller, which reflects the expected responses within the excitation range. The seismic response of the VG system consistently demonstrated stability and similarity between the original and repeated testing sessions. The DAF presented in Table 3 indicated favourable relationships between the response and input peak acceleration values.

Overall, the obtained acceleration histories, alongside the absolute displacement data monitored by LP sensors on the sub- and superstructure segments, showed strong correlation across all tests confirming the successful completion of the comprehensive testing program.

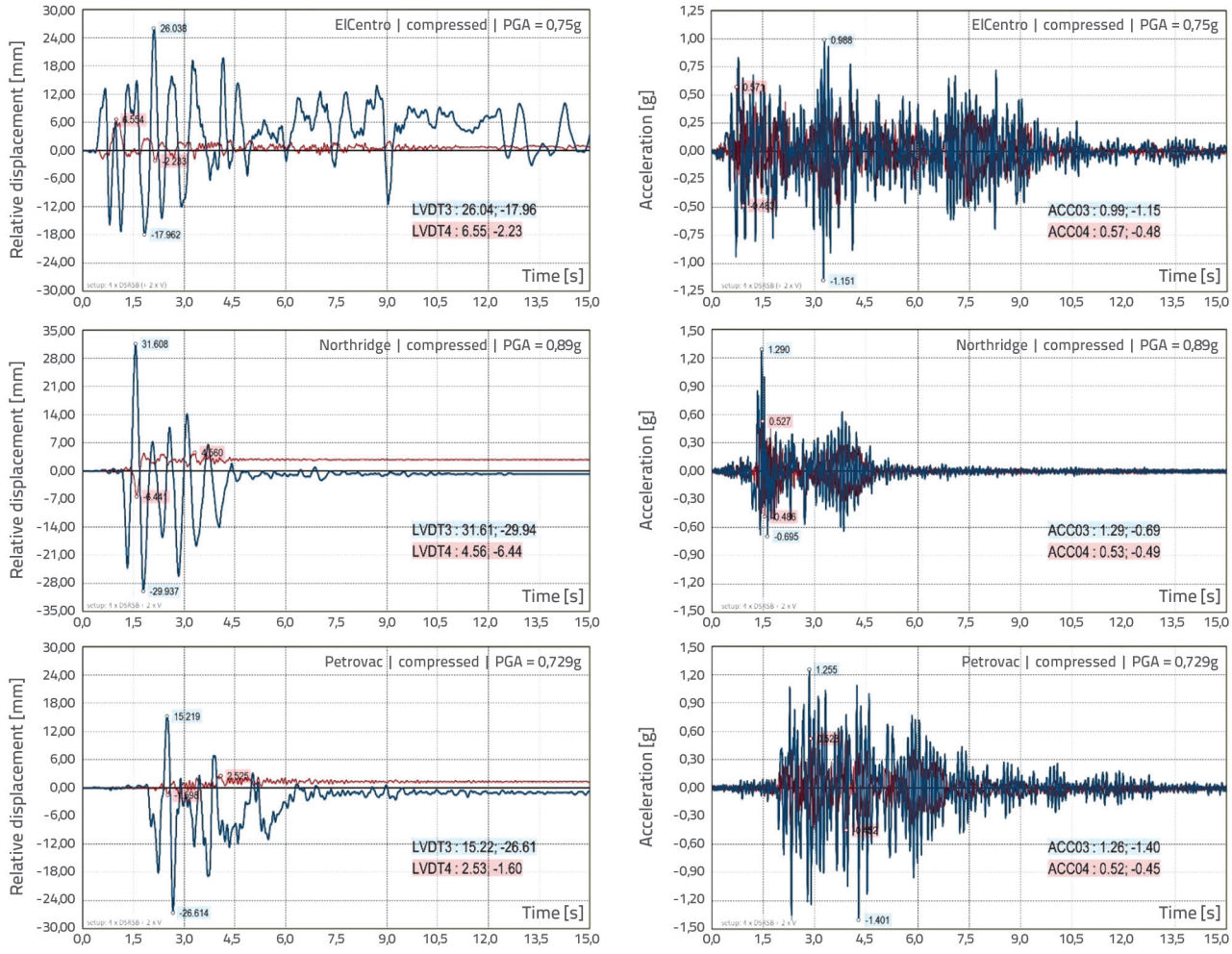

Figure 14. Relative superstructure displacement responses recorded by LVDT-03 & LVDT-04 (left) and acceleration responses recorded by ACC-03 and ACC-04 (right) during the shaking table tests conducted with simulated strong El-Centro, Northridge, and Petrovac earthquakes

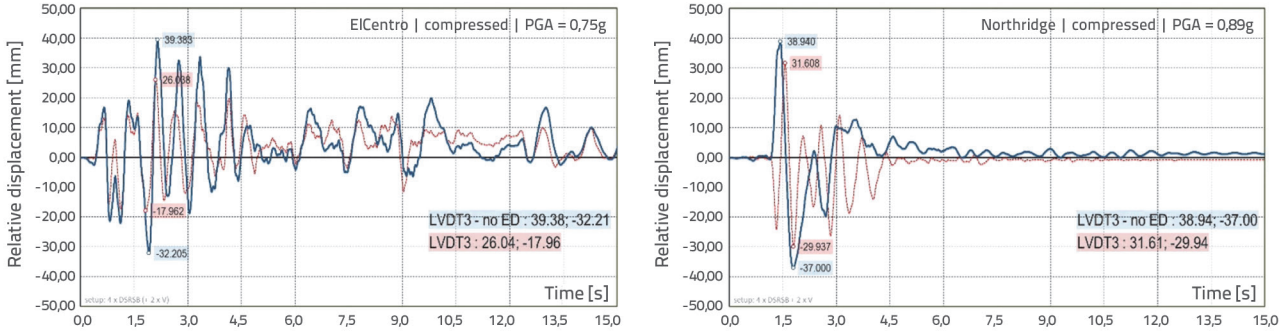

Figure 15. Comparison of the relative displacements of the VG system without (blue lines, predicted) and with ED devices (red lines, recorded): El-Centro record PGA = 0.78 g (left) and Northridge record PGA = 0.89 g (right), assuming the FEM model node consistent with the LVD3 location

As shown in Figure 16, the contribution of energy dissipation devices to the structural response is evaluated by testing a bridge model equipped with only four DSRSB isolators (without dissipaters) on a shaking table under simulated El Centro excitation scaled to PGA 0.78 g. In addition, an analytical study of the bridge response was conducted considering isolated bridges with and without V-MG energy dissipation devices. Figure 15 illustrates the comparison of relative displacements

between the system without (blue lines) and with V-MG devices (red lines) under El-Centro PGA = 0.78 g and Northridge PGA = 0.89 g records.

The comparisons highlight the effectiveness of V-MG energy-dissipation devices in reducing structural displacements and enhancing seismic performance compared with that of isolated configurations relying solely on DSRSB isolators.

6. Observations from the VG bridge model tests

As shown in Figure 16, the effectiveness of reducing the maximum relative displacement in the bridge superstructure with the VG bridge system, including the newly implemented V-MG devices, was confirmed through seismic shaking-table tests of the prototype model under very strong simulated earthquakes. Significant reductions in the maximum responses were observed across all test cases. Compared with the defined maximum allowable displacement of 40 mm for seismic isolators, the peak responses for the El Centro (0.78 g), Petrovac (0.72 g), Landers (0.76 g), and Northridge (0.89 g) earthquakes were reduced by 34.9, 33.5, 49.1, and 20.9%, respectively. The tests demonstrated stable, reliable, and safe seismic responses with the maximum displacements consistently controlled below the limit.

An additional comparative shaking table test was conducted on the assembled prototype model without V-MG devices (seismic isolation only) to further understand the effect of the V-MG devices on the bridge response. A significantly increased maximum relative displacement response of 42.31 mm was recorded using the same El Centro earthquake intensity (0.78 g) as the input. As indicated in Figure 16, this exceeds the allowable displacement of 40.0 mm for the seismic isolators, which indicates the potential for intolerable damage consequences caused by the unsafe bridge response.

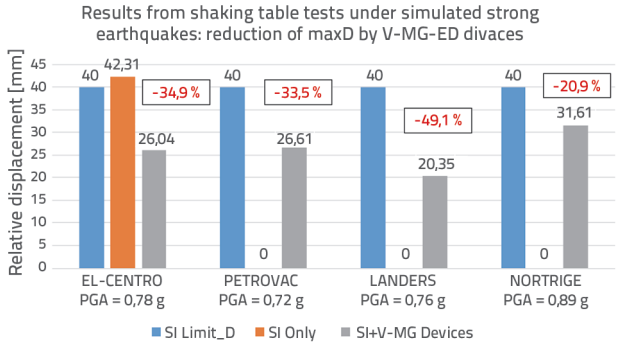

Figure 16. Reduction of the maximum relative displacement with the installed new V-MG devices was confirmed with the conducted seismic tests on the VG bridge model under simulated strong earthquakes

The study demonstrated that the method developed for upgrading isolated bridges with novel V-gapped devices resulted in a significantly improved bridge performance and safe response during strong earthquakes. The installed V-MG devices exhibited the potential to effectively protect bridges, even under stronger future seismic events. This indicates that the upgraded system with V-MG devices enhances the seismic resilience and safety of bridges subjected to high-intensity earthquakes.

7. Conclusions

Extensive experimental and theoretical studies conducted to develop a method for upgrading isolated bridges using novel V-gapped devices yielded several key conclusions:

- VG systems, which integrate seismic isolation, energy dissipation, and displacement control, have proven to be highly effective for the seismic protection of bridges. Its adaptive ductile seismic response renders it suitable for protecting bridges from repeatedly strong earthquakes.
- DSRSB devices were validated as a suitable choice for creating a seismic isolation system and have the potential for integration into more complex, multilevel seismic protection systems such as the VG system. Other isolation devices such as rubber isolators can be considered as alternatives.
- Uniform V-MG energy-dissipation devices demonstrated excellent energy absorption capabilities with stable hysteretic behaviour under various earthquake conditions, which includes intensive repeated cyclic loading.
- Displacement–limiting (DL) devices are essential components of VG systems and provide crucial protection against excessive displacement of the bridge superstructure. Their activation significantly improves the seismic safety of bridges during critical displacement events.
- The gap-based hysteretic behaviour of V-MG components and integrated devices can be accurately predicted using advanced microanalytical models employing bilinear kinematic hardening material models.
- The results of extensive experimental and analytical studies provided essential data for developing validated finite element method (FEM) analytical models. These models are crucial for the practical design of bridges equipped with advanced VG seismic protection systems. This study demonstrated that a VG system offers robust seismic protection capabilities by combining isolation, energy dissipation, and displacement control for enhancing the resilience of bridges against strong earthquakes.

Acknowledgements

The research was realised at the Institute of Earthquake Engineering and Engineering Seismology, "Ss Cyril & Methodius" University, Skopje, in the frame of the NATO Science for Peace and Security Innovative Project: Seismic Upgrading of Bridges in South-East Europe by Innovative Technologies (SFP: 983828) with the participation of five countries: North Macedonia: D. Ristic, Leader & PPD-Director, Germany: U. Dorka, NPD-Director, Albania: A. Lako, Bosnia & Herzegovina: D. Zenunovic & Serbia: R. Folic. The extended support to the realisation of the project is highly appreciated.

REFERENCES

[1] Kelly, J.M.: Aseismic Base Isolation: A Review and Bibliography, Soil Dynamics and Earthquake Engineering, 5 (1986), pp. 202-216.

[2] Kunde, M.C., Jangid, R.S.: Seismic Behaviour of Isolated Bridges: A-State-of-the-art Review, Electronic Journal of Structural Engineering, 3 (2003), pp. 140-170.

[3] Turkington, D.H., Carr, A.J., Cooke, N., Moss, P.J.: Seismic Design of Bridges on Lead–Rubber Bearings, Journal of Structural Engineering, 115 (1989), pp. 3000-3016.

[4] Robinson, W.H.: Lead-Rubber Hysteretic Bearings Suitable for Protecting Structures During Earthquakes, Earthquake Engineering and Structural Dynamics, 10 (1982), pp. 593-604.

[5] Dolce, M., Cardone, D., Palermo, G.: Seismic Isolation of Bridges Using Isolation Systems Based on Flat Sliding Bearings, Bulletin of Earthquake Engineering, 5 (2007), pp. 491–509.

[6] Iemura, H., Taghikhany, T., Jain, S.K.: Optimum Design of Resilient Sliding Isolation System for Seismic Protection of Equipment, Bulletin of Earthquake Engineering, 5 (2007), pp. 85–103.

[7] Kartoum, A., Constantinou, M.C., Reinhorn, A.M.: Sliding Isolation System for Bridges: Analytical Study, Earthquake Spectra, 8 (1992), pp. 345-372.

[8] Wang, Y.P., Chung, L., Wei, H.L.: Seismic Response Analysis of Bridges Isolated with Friction Pendulum Bearings. Earthquake Engineering and Structural Dynamics, 27 (1998).

[9] Zayas, V.A., Low, S.S., Mahin, S.A.: A Simple Pendulum Technique for Achieving Seismic Isolation, Earthquake Spectra, 6 (1990), pp. 317-334.

[10] Mokha, A., Constantinou, M.C., Reinhorn, A.M.: Teflon Bearings in Seismic Base Isolation I: Testing, Journal of Structural Engineering, 116 (1990), pp. 438-454.

[11] Constantinou, M.C., Kartoum, A., Reinhorn, A.M., Bradford, P.: Sliding Isolation System for Bridges: Experimental study. Earthquake Spectra, 8 (1992), pp. 321-344.

[12] Xiang, N., Yang, H., Li, J.: Performance of an Isolated Simply Supported Bridge Crossing Fault Rupture: Shake Table Test, Earthquakes and Structures, 16 (2019) 6.

[13] Skinner, R.I., Kelly, J.M., Heine, A.J.: Hysteretic Dampers for Earthquake Resistant Structures, Earthquake Engineering and Structural Dynamics, 3 (1975), pp. 287-296.

[14] Guan Z., Li J., Xu, Y.: Performance Test of Energy Dissipation Bearing and Its Application in Seismic Control of a Long-Span Bridge, Journal of Bridge Engineering, 15 (2010).

[15] Javanmardi, A., Ibrahim, Z., Ghaedi, K., Ghadim, H.B., Hanif, M.U.: State-of-the-Art Review of Metallic Dampers: Testing, Development and Implementation. Archives of Computational Methods in Engineering, 27 (2020), pp. 455–478.

[16] Ene, D., Yamada, S., Jiao, Y., Kishiki, S., Konishi. Y.: Reliability of U-shaped Steel Dampers Used in Base-Isolated Structures Subjected to Biaxial Excitation, Earthquake Engineering Structural Dynamics, 46 (2017), pp. 621–639.

[17] Oh, S., Song, S., Lee, S., Kim, H.: Experimental Study of Seismic Performance of Base-Isolated Frames with U-shaped Hysteretic Energy-Dissipating Devices, Engineering Structures, 56 (2013), pp. 2014-2027.

[18] Jiao, Y., Kishiki, S., Yamada, S., Ene, D., Konishi, Y., Hoashi, Y., Terashima, M.: Low Cyclic Fatigue and Hysteretic Behaviour of U-Shaped Steel Dampers for Seismically Isolated Buildings Under Dynamic Cyclic Loadings. Earthquake Engineering Structural Dynamics, 44 (2014) 10, pp. 1523–1538.

[19] Tyler, R.G.: Tapered Steel Energy Dissipators for Earthquake-Resistant Structures; Bulletin of the New Zealand National Society for Earthquake Engineering, 11 (1978), pp. 282–294.

[20] Ghaedi, K., Ibrahim, Z., Javanmardi, A.: New Metallic Bar Damper Device for Seismic Energy Dissipation of Civil Structures. U: IOP Conference Series: Materials Science and Engineering, IOP Publishing, 431 (2018) 12, 122009.

[21] Briones, B., de la Llera, J.C.: Analysis, design, and testing of an hourglass-shaped ETP-copper energy-dissipation device. Eng Struct, 79 (2014), pp. 309–321

[22] Sepúlveda, J., Boroschek, R., Herrera, R., Moroni, O., Sarrazin, M.: Steel Beam-Column Connection Using Copper-Based Shape Memory Alloy Dampers. Journal of Constructional Steel Research, 64 (2008), pp. 429–435.

[23] Jankowski, R., Seleemah, A., El-Khoribi, S., Elwardany, H.: Experimental Study on Pounding between Structures During Damaging Earthquakes, Key Engineering Materials, 627 (2015), pp. 249–252.

[24] Tubaldi, E., Mitoulis, S.A., Ahmadi, H., Muhr, A.: A Parametric Study on the Axial Behaviour of Elastomeric Isolators in Multispan Bridges Subjected to Horizontal Seismic Excitations, Bulletin of Earthquake Engineering, 14 (2016), pp. 1285–1310.

[25] Serino, G., Occhiuzzi, A.: A Semi-Active Ododynamic Damper for Earthquake Control Part 1: Design, Manufacturing and Experimental Analysis of the Device. Bulletin of Earthquake Engineering, 1 (2003), pp. 269–301.

[26] Kataria, N.P., Jangid, R.S.: Seismic Protection of the Horizontally Curved Bridge with Semi-Active Variable Stiffness Damper and Isolation System, Advances in Structural Engineering, 19 (2016) 7, pp. 1103–1117.

[27] Mayes, R.L., Buckle, I.G., Kelly, T.E., Jones, L.R.: AASHTO Seismic Isolation Design Requirements for Highway Bridges, Journal of Structural Engineering, 118 (1992), pp. 284-304.

[28] NHI.: LRFD Seismic Analysis and Design of Bridges, Reference Manual: NHI Course Nos. 130093 and 130093A, National Highway Institute, U.S. Department of Transportation, 2014.

[29] Unjoh, S., Ohsumi, M.: Earthquake Response Characteristics of Super-Multispan Continuous Menshin (seismic isolation) Bridges and the Seismic Design, ISET Journal of Earthquake Engineering Technology, 1998, 35, 95–104.

[30] Tian, L., Fu, Z., Pan, H., Ma, R., Liu, Y.: Experimental and Numerical Study on the Collapse Failure of Long-Span Transmission Tower-Line Systems Subjected to Extremely Severe Earthquakes, Earthquakes and Structures, 16 (2019) 5.

[31] UNCRD.: Comprehensive Study of the Great Hanshin Earthquake, UNCRD Research Report Series No. 12, United Nations Centre for Regional Development (UNCRD), Nagoya, Japan, 1995).

[32] Lin, C.C.J., Hung, H.H., Liu, K.Y., Chai, J.F.: Reconnaissance Observation on Bridge Damage Caused by the 2008 Wenchuan (China) Earthquake, Earthquake Spectra, 26 (2010).

[33] Guo, W., Gao X., Hu P., et al.: Seismic Damage Features of High-Speed Railway Simply Supported Bridge–Track System under Near-Fault Earthquake, Advances in Structural Engineering, 23 (2020), pp. 1–14.

[34] NIST: 17 January 1995 Hyogoken-Nanbu (Kobe) Earthquake: Performance of Structures, Lifelines, and Fire Protection Systems, NIST SP 901, U.S. Department of Commerce, Technology Administration, Washington, USA, 1996.

[35] Yuan, W., Feng, R., Dang, X.: Typical Earthquake Damage and Seismic Isolation Technology for Bridges Subjected to Near-Fault Ground Motions, 2018 International Conference on Engineering Simulation and Intelligent Control, August 2018., Hunan, China, 2018.

[36] Aye, M., Kasai, A., Shigeishi, M.: An Investigation of Damage Mechanism Induced by Earthquake in a Plate Girder Bridge Based on Seismic Response Analysis: Case Study of Tawarayama Bridge under the 2016 Kumamoto Earthquake, Advances in Seismic Performance Assessment and Improvement of Structures, 2018.

[37] Lee, G.C., Lee, Y., Kitane, I.G.: Literature Review of the Observed Performance of Seismically Isolated Bridges, Multidisciplinary Center for Earthquake Engineering Research, New York, NY, USA, 2001.

[38] Ghasemi, H., Cooper, J.D., Imbsen, R., Piskin, H., Inal, F., Tiras, A.: The November 1999 Duzce Earthquake: Post-Earthquake Investigation of the Structures on the TEM. FHWA-RD-00-146, Federal Highway Administration Report, 2000.

[39] Erdik, M.: Report on 1999 Kocaeli and Duzce (Turkey). Earnual, Structural Control for Civil and Infrastructure Engineering, (2001), pp. 149–186.

[40] Fujino, Y., Siringoringo, D.M., Kikuchi, M., Kasai, K., Kashima, T.: Seismic Monitoring of Seismically Isolated Bridges and Buildings in Japan—Case Studies and Lessons Learned; In: Limongelli M., Çelebi M. (eds) Seismic Structural Health Monitoring, Springer Tracts in Civil Engineering, Springer, Cham, 2019.

[41] Li, X., Shi, Y.: Seismic Design of Bridges Against Near-Fault Ground Motions using Combined Seismic Isolation and Restraining Systems of LRBs and CDRs. 2019, Article ID 4067915, 11.

[42] Zlatkov, D., Ristic, D., Zoric, A., Ristic, J., Mladenovic, B., Petrovic, Z., Trajkovic-Milenkovic, M.: Experimental and Numerical Study of Energy Dissipation Components of a New Metallic Damper Device, Journal of Vibration Engineering & Technologies, 2022.

[43] Ristic, J., Misini, M., Ristic, D., Guri, Z., Pllana, N.: Seismic upgrading of isolated bridges with SF-ED devices:Shaking table tests on large-scale model, GRAĐEVINAR, 70 (2018) 6, pp. 463-485, https://doi.org/10.14256/JCE.2147.2017

[44] Ristic, J., Ristic, D., Hristovski, V.: Upgrading of Isolated Bridges with Uniform Gapped HS Devices: Seismic Tests, GRAĐEVINAR, 74 (2022) 12, pp. 1047–1058. https://doi.org/10.14256/JCE.3580.2022

[45] Misini, M., Ristic, J., Ristic, D., Guri, Z., Pllana, N.: Seismic Upgrading of Isolated Bridges with SF-ED Devices: Analytical Study Validated by Shaking Table Testing, GRAĐEVINAR, 71 (2019) 4, pp. 255–272. https://doi.org/10.14256/JCE.2274.2017

[46] Ristic, J., Brujic, Z., Ristic, D., Folic, R., Boskovic, M.: Upgrading of Isolated Bridges with Space-Bar Energy-Dissipation Devices: Shaking Table Test, Advances in Structural Engineering, 2021, pp. 2948–2965.

[47] Ristic, J.: Modern Technology for Seismic Protection of Bridge Structures Applying Advanced System for Modification of Earthquake Response, PhD Thesis, Institute of Earthquake Engineering and Engineering Seismology (IZIIS), "SS Cyril and Methodius" University, Skopje, Macedonia, 2016.

[48] Candeias, P., Costa, A.C., Coelho, E.: Shaking Table Tests of 1:3 Reduced Scale Models of Four-Story Unreinforced Masonry Buildings, 13th World Conference on Earthquake Engineering, 2004, Vancouver, Paper: 2199.